

Selective PPAR δ Modulators Improve Mitochondrial Function:
Potential Treatment for Duchenne Muscular Dystrophy (DMD)

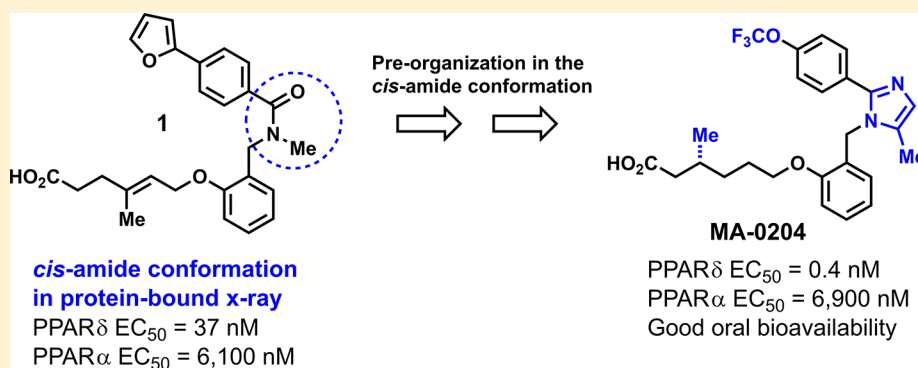
Bharat Lagu,^{*,†,‡} Arthur F. Kluge,[†] Effie Tozzo,[†] Ross Fredenburg,[†] Eric L. Bell,[†] Matthew M. Goddeeris,[†] Peter Dwyer,[†] Andrew Basinski,[†] Ramesh S. Senaiar,[‡] Mahaboobi Jaleel,[‡] Nirbhay Kumar Tiwari,[‡] Sunil K. Panigrahi,[‡] Narasimha Rao Krishnamurthy,[‡] Taisuke Takahashi,[§] and Michael A. Patane[†]

[†]Mitobridge, Inc. (a wholly owned subsidiary of Astellas Pharma.), 1030 Massachusetts Avenue, Cambridge, Massachusetts 02138, United States

[‡]Aurigene Discovery Technologies, Ltd., Bengaluru and Hyderabad, India

[§]Astellas Pharma., Tsukuba, Japan

S Supporting Information



ABSTRACT: The X-ray structure of the previously reported PPAR δ modulator **1** bound to the ligand binding domain (LBD) revealed that the amide moiety in **1** exists in the thermodynamically disfavored *cis*-amide orientation. Isosteric replacement of the *cis*-amide with five-membered heterocycles led to the identification of imidazole **17** (MA-0204), a potent, selective PPAR δ modulator with good pharmacokinetic properties. MA-0204 was tested *in vivo* in mice and *in vitro* in patient-derived muscle myoblasts (from Duchenne Muscular Dystrophy (DMD) patients); **17** altered the expression of PPAR δ target genes and improved fatty acid oxidation, which supports the therapeutic hypothesis for the study of MA-0204 in DMD patients.

KEYWORDS: PPAR δ modulators, Duchenne Muscular Dystrophy (DMD), mdx mouse, imidazoles, *cis*-amide

Duchenne Muscular Dystrophy (DMD) is an X-linked recessive genetic disease involving severe muscle wasting that results from cycles of muscle degeneration/regeneration.^{1,2} DMD patients carry mutations in the DMD gene, which encodes for dystrophin, a cellular protein scaffold that is critical for muscle membrane integrity.³ In addition to weakened structural integrity, DMD is also characterized by mitochondrial impairment with evidence of decreased fatty acid oxidative phosphorylation.^{4–7}

In skeletal muscle, PPAR δ elicits a transcriptional cascade resulting in increased fatty acid oxidation while sparing glucose utilization, which enables muscle to function for a longer duration without decreasing systemic glucose levels or increasing muscle lactic acid.⁸ We hypothesized that engaging the PPAR δ transcriptional cascade with a selective PPAR δ modulator would provide functional improvements to DMD muscle.

The selectivity for PPAR δ is considered to be crucial to mitigate the undesirable effects (such as hepatotoxicity, myopathy, edema, cardiac toxicity, etc.) observed with some modulators of PPAR α (fibrates), PPAR γ (thiazolidinediones), and dual PPAR α/γ (e.g., Muraglitazar) in clinical and/or preclinical studies,^{9,10} while GW501516,¹¹ a known PPAR δ modulator, has shown tumorigenic effects in mice.¹² As per the company Web sites, two modulators of PPAR δ , Seladelpar and Elafibranor, have cleared the two-year carcinogenicity studies in rats. This suggests that tumorigenic potential is not a class effect for the PPAR modulators.

We recently disclosed the potent and selective PPAR δ modulator **1** (Figure 1), which displayed significantly improved

Received: June 23, 2018

Accepted: July 31, 2018

Published: July 31, 2018



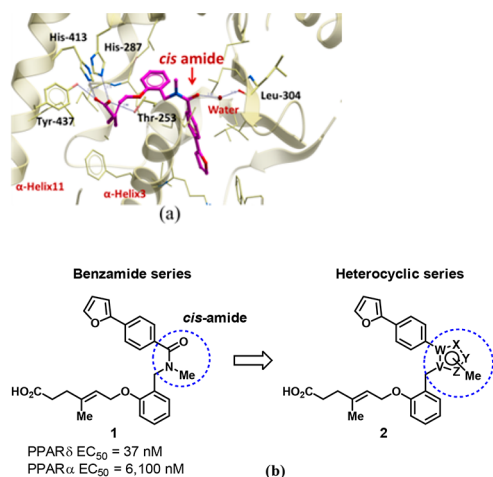


Figure 1. (a) X-ray structure of **1** bound to PPAR δ LBD. (b) Isosteric replacement of *cis*-amide with five-membered heterocycles.

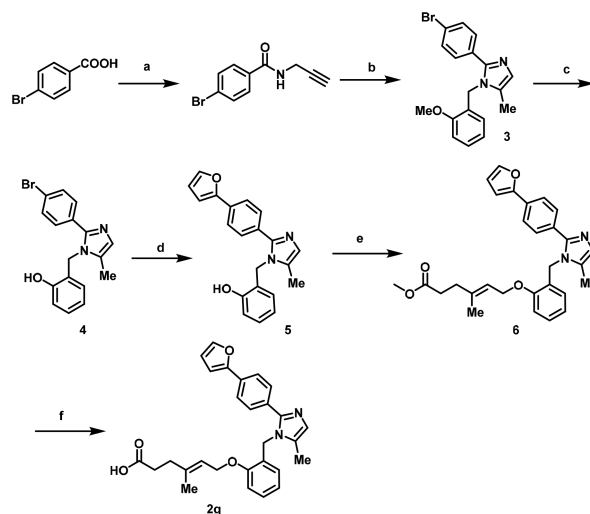
pharmacokinetic properties relative to previously reported compounds.^{13–15} The X-ray structure of **1** bound to the ligand binding domain (LBD) of the PPAR δ receptor revealed that the carbonyl oxygen and the *N*-methyl group are in a *cis* relationship.¹³ A *trans*-amide has been reported to be thermodynamically favored over a *cis*-amide.¹⁶ *Cis*-Amides are uncommon even in the peptide literature, especially for amino acids other than proline.¹⁷ Molecular mechanics-based energy minimization and conformational analysis of **1** predicted that the *trans* isomer is favored by 1.3 kcal/mol over the *cis* isomer.¹⁸ Therefore, we reasoned that a molecule in a “locked *cis*-amide” conformation would improve binding affinity for PPAR δ . Herein, we disclose a series of compounds represented by general structure **2**, where five-membered heterocyclic rings (Figure 1) serve as isosteric replacements of the *cis*-amide bond.

The heterocyclic cores required for compounds **2a–g** were synthesized using known synthetic procedures (see Supporting Information for the detailed procedures). Synthesis of **2g** is shown in Scheme 1 as a representative example.

PPAR δ , PPAR α , and PPAR γ activities of these compounds were assessed using transactivation assays.¹⁹ All the compounds were screened for exposure in mice following an intravenous dose of 3 mg/kg. The results are shown in Table 1.

All of the heterocyclic compounds (except compound **2f**) in Table 1 show greater affinity ($EC_{50} < 10$ nM) for PPAR δ receptor than the original amide lead **1**, supporting our hypothesis regarding the use of heterocycles as *cis*-amide isosteres. All the compounds were found to selectively activate PPAR δ (>1000-fold less potent for PPAR α and PPAR γ receptors). Unlike compound **1**, all the compounds (except **2b**) shown in Table 1 have plasma clearances that exceed hepatic blood flow in mice (>85 mL/min/kg), short half-lives (<1 h), and low plasma exposures (AUC <1000 ng·h/mL) when dosed intravenously in mice. Compound **2b** has the highest plasma exposure among the compounds shown in Table 1 but is 5–10-fold less potent for PPAR δ compared to the remaining compounds. Although **2d** and **2g** showed comparable PPAR δ activity and plasma clearance values, imidazole **2g** was selected for further optimization based on the superior solubility properties (data not shown). Our previous work in the benzamide series (like compound **1**) demonstrated that modifications of the hexanoic acid side chain significantly influence the observed pharmacokinetic (PK) properties.^{13,14}

Scheme 1. Synthesis of Compound **2g**^a



^aReagents and conditions: (a) Prop-2-yn-1-amine, EDCI·HCl, HOBT, Et₃N, DMF, RT; (b) (2-methoxyphenyl)methanamine, Zn(OTf)₂, toluene, MW (irradiation), 140 °C; (c) BBr₃, DCM, RT; (d) furan-2-boronic acid, Pd(PPh₃)₄, Na₂CO₃, DME, EtOH, H₂O, 90 °C; (e) methyl (*E*)-6-bromo-4-methylhex-4-enoate, K₂CO₃, DMF, 65 °C; (f) LiOH·H₂O, THF, EtOH, H₂O, RT.

Therefore, similar chemistry exploration was undertaken in the imidazole series (e.g., **2g**). Compounds **13–22** were synthesized as shown in Scheme 2. The results of pharmacological and pharmacokinetic studies are summarized in Table 2.

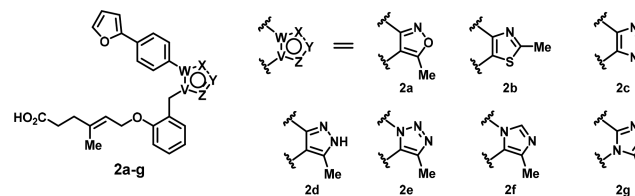
In general, PPAR δ activity was significantly better for imidazole series of compounds (e.g., PPAR δ EC_{50} = 37 nM for **1** compared to PPAR δ EC_{50} = 1 nM for **2g**). However, higher plasma exposures were observed for the compounds in the benzamide series compared to the imidazole series (e.g., AUC = 3300 ng·h/mL for **1** compared to 300 ng·h/mL for **2g**). A significant improvement in plasma clearance and plasma exposures was observed when the hexanoic acid region included substitutions at α , β , and γ positions relative to the carboxylic acid (e.g., **2g**, **14**, and **15** compared to **13**). A similar trend in the pharmacokinetic properties was observed for the benzamide series of compounds.

Among the substituents tried as a replacement of the 2-furyl moiety (compounds **17–22**), 4-trifluoromethoxy group containing compound **17** stood out based on subnanomolar activity for PPAR δ , good selectivity over the other PPAR subtypes, reduced plasma clearance, and improved plasma exposure.

An X-ray structure of compound **13** bound to the LBD of PPAR δ (Figure 2) was obtained at 2 Å resolution.²¹ As anticipated, the imidazole ring in **13** superimposes nicely with the *cis*-amide bond in the protein bound X-ray structure of **1**. Almost all the interactions observed between **1** and the protein (His287, His413, Thr253, and Tyr437) are conserved in the X-ray structure for **13**. One of the nitrogen atoms in the imidazole ring of **13** forms a water-mediated interaction with Leu304 as was observed for the *cis*-amide in the X-ray structure for **1**.¹³

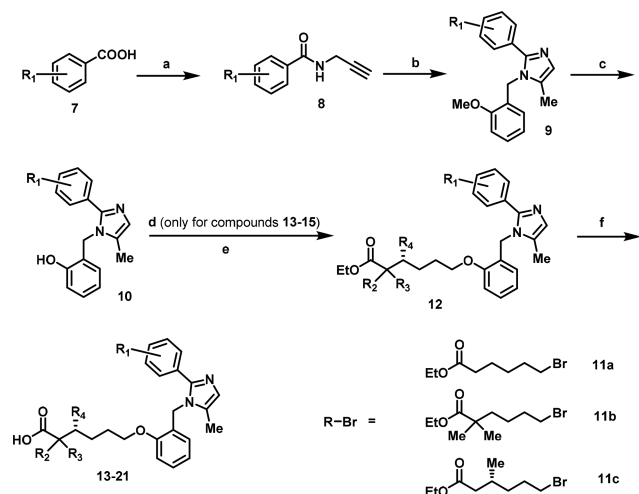
The binding interactions with Val312 and Ile328 have been postulated to impart selectivity for a known PPAR δ selective modulator, GW0742.²² Overlay of the crystal structures of **13** with GW0742 (PDB ID: 3TKM) reveals a significant downward movement of the Ile328 residue in the structure

Table 1. Structure–Activity Relationship in the Five-Membered Heterocyclic Series



Cpd	PPAR δ EC ₅₀ (nM) ^a	PPAR α EC ₅₀ (nM) ^{a,b}	<i>t</i> _{1/2} (h) ^c	CL (mL/min/kg) ^c	AUC (ng·h/mL) ^c
1	37 ± 5	6100	2.3	15	3300
2a	1.5	5840	0.2	180	280
2b	9.5 ± 0.5	7250	0.8	55	900
2c	1.3 ± 0.5	412 ± 7.1	0.8	300	170
2d	1.2	13100	0.4	130	380
2e	8.4 ± 1.4	16800	0.2	225	220
2f	59 ± 3.6	ND	0.7	720	70
2g	1.0 ± 0.0	1230 ± 165	0.5	160	300

^aTransactivation assay.¹⁹ In selected cases, compounds were also assayed in a protein interaction assay.²⁰ Both assays were in good agreement. EC₅₀ values are an average of at least two experiments (SEM shown unless single determination). ^bAll the compounds, except 2d, showed EC₅₀ >10 000 nM for PPAR γ ; PPAR γ EC₅₀ for 2d = 5530 nM; ^cExposure data for compounds dosed i.v. at 3 mg/kg to CD-1 mice; ND = not determined.

Scheme 2. General Synthesis of Compounds 13–22^a

^aReagents and conditions: (a) prop-2-yn-1-amine, EDCI·HCl, HOBT, Et₃N, DMF, RT; (b) (2-methoxyphenyl)methanamine, Zn(OTf)₂, toluene, microwave irradiation, 140 °C; (c) BBr₃, DCM, RT; (d) for compounds 13–15: furan-2-boronic acid, Pd(PPh₃)₄, Na₂CO₃, DME, EtOH, H₂O, 90 °C; (e) R-Br (11a or 11b or 11c), K₂CO₃, DMF, 65 °C; (f) LiOH·H₂O, THF, EtOH, H₂O, RT.

for 13, even though the Val312 conformation is conserved in both structures. This movement is possibly necessitated by the presence of the benzyl moiety on the imidazole ring. Ile328 in PPAR δ is replaced by methionine residues in PPAR α and PPAR γ . Changes in the Ile328 region and the water-mediated interaction with Leu304 potentially contribute to the improved PPAR δ selectivity for the imidazole series of compounds.

Compound 17 was profiled in multiple *in vitro* and *in vivo* assays (Table 3). Compound 17 is >10 000-fold selective for activation of PPAR δ over PPAR α and PPAR γ receptors. The PPAR δ potency was 10-fold less for mouse and rat PPAR δ receptors than for the human PPAR δ receptor; this effect is well documented for PPAR modulators.¹¹ Compound 17 is selective (EC₅₀ >10 μ M) over other nuclear receptors, for example:

androgen, progesterone, and glucocorticoid receptors. Compound 17 is also inactive in a panel of 68 receptors and transporters that are known to pose safety-related challenges in the clinic. Compound 17 exhibits high protein binding to mouse plasma, good permeability, and low potential for efflux. Compound 17 did not show mutagenic potential or inhibit major cytochrome P450 enzymes (IC₅₀ ≥10 μ M). Compound 17 has acceptable PK profiles in mice and rats upon oral dosing.²³ In the aggregate, these properties made 17 (MA-0204) an excellent candidate for study in pharmacological assays.

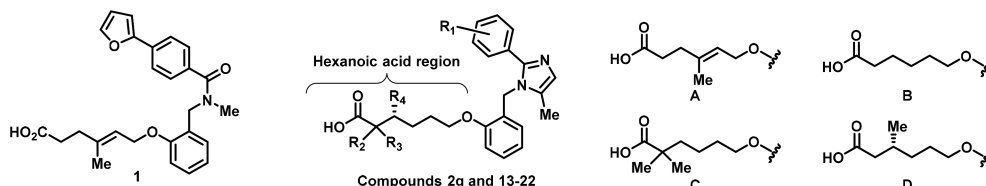
For compound 17 (MA-0204) to be considered as a potential treatment for Duchenne Muscular Dystrophy (DMD), it was necessary to demonstrate that it met at least three criteria: (1) elicit a response in the target tissue, i.e., skeletal muscle, (2) affect changes in the PPAR δ -responsive genes in DMD patient myoblasts, and (3) affect beta oxidation of fatty acid in patient myoblasts. The results from these *in vivo* and *ex vivo* experiments are described below.

To determine if 17 was capable of eliciting a biological effect in skeletal muscle, mice were dosed orally with MA-0204 and GW501516, and target gene expression was assessed by qPCR (quantitative polymerase chain reaction). As shown in Figure 3, 17 increased PPAR δ target gene transcription in the muscle, represented here by *Pdk4* (pyruvate dehydrogenase kinase 4).

In order to test for changes in fatty acid oxidation, primary myoblasts isolated from a 17-month-old DMD patient were utilized. Compound 17 increased PPAR δ target genes *ANGPTL4* (angiopoietin like protein 4), *CPT1a* (carnitine palmytoyltransferase 1a), and *PDK4* in a dose-dependent manner (Figure 4). Furthermore, oxidation of the long-chain fatty acid palmitic acid was significantly elevated at the concentrations of 1.2, 4, and 12 nM (3-, 10-, and 30-fold EC₅₀, respectively), which represents a functional improvement of up to 52% in palmitate utilization (Figure 5).

In summary, we have reported the design and synthesis of a series of potent and selective PPAR δ modulators by utilizing X-ray crystallographic information derived from previously disclosed compounds. The key compound to emerge from these studies, 17 (MA-0204), combined potency and PK properties, which enabled the demonstration that selective PPAR δ

Table 2. Hexanoic Acid Region Modifications, PPAR Activity, and Selected Pharmacokinetic Data



Cpd	R ₁	hexanoic acid region modifications	PPAR δ EC ₅₀ (nM) ^a	PPAR α EC ₅₀ (nM) ^a	t _{1/2} (h) ^b	CL (mL/min/kg) ^b	AUC (ng·h/mL) ^b
1			37 ± 5	6100	2.3	15	3300
2g	4-(2-furyl)	A	1.0 ± 0.0	1230 ± 165	0.5	160	300
13	4-(2-furyl)	B	0.7 ± 0.2	6970	0.3	270	180
14	4-(2-furyl)	C	4.5	ND	2.4	120	400
15	4-(2-furyl)	D	3.7 ± 0.1	>100000	1.4	73	650
16	OCF ₃	A	0.3 ± 0.1	2290	3.1	70	240 ^c
17	4-OCF ₃	D	0.4 ± 0.1	6900 ± 1030	3.3	25	1250
18	4-Cl-3-F	D	0.8 ± 0.1	69000	4.3 ^c	38 ^c	440 ^c
19	4-Cl	D	5.5 ± 2.8	>100000	1.4 ^c	22 ^c	752 ^c
20	4-Me	D	20 ± 4.8	78500	ND	ND	ND
21	4-OCHF ₂	D	13.5	15060	ND	ND	ND
22	4-F	D	39.0	>100000	ND	ND	ND

^aTransactivation assay.¹⁹ In selected cases, compounds were also assayed in a protein interaction assay.²⁰ Both assays were in good agreement. EC₅₀ values are an average of at least two experiments (SEM shown unless single determination). ^bExposure data for compounds dosed i.v. at 3 mg/kg to CD-1 mice. ^cExposure data for compounds dosed i.v. at 1 mg/kg to CD-1 mice. ND = not determined. All the compounds showed EC₅₀ > 10000 nM for PPAR γ .

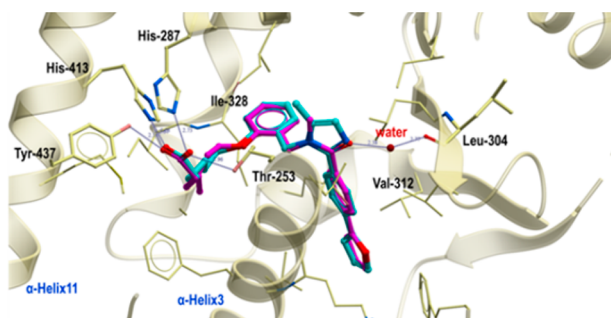


Figure 2. Superposition of the X-ray structures of compound 1 (magenta) and compound 13 (cyan) bound to the ligand binding domain (LBD) of PPAR δ receptor.

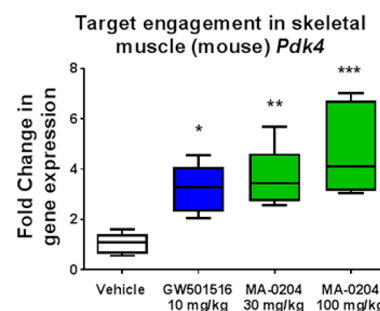


Figure 3. Compound 17 (MA-0204) engages target gene expression after oral administration in mice (see Supporting Information for details).

Table 3. Potency, Selectivity, ADME, DMPK, PK, and Safety Data for 17 (MA-0204)

assay	results
human PPAR δ	EC ₅₀ = 0.4 nM ^a
human PPAR α and PPAR γ	EC ₅₀ = 6990 ± 1030 nM and >100 000 nM, respectively ^a
mouse PPAR δ and Rat PPAR δ	EC ₅₀ = 7.9 nM and 10 nM ^b
selectivity	no activity in Eurofins PanLabs Lead Profiling Screen of 68 molecular targets up to 10 μ M. No activity (up to 10 μ M) for androgen, progesterone, and glucocorticoid receptors ^c
% plasma protein binding:	mouse/rat/human = 99.5/99.6/99.9
Caco-2 permeability (cm/s, $\times 10^{-6}$)	A to B = 36; B to A = 41 (efflux ratio 1.2)
CYP450 inhibition	>10 μ M for CYPs except 2C9 (56% inhibition @ 10 μ M)
mutagenicity	nonmutagenic in mini-Ames test
mouse PK ^d	1 mg/kg IV: t _{1/2} = 2.7 h; CL = 33 mL/min/kg; V _{ss} = 5.8 L/kg; AUC = 503 ng·h/mL 3 mg/kg PO: t _{1/2} = 3.4 h; C _{max} = 510 ng/mL; AUC = 630 ng·h/mL; %F = 42
rat PK ^e	1 mg/kg IV: t _{1/2} = 6.1 h; V _{ss} = 1.8 L/kg; CL = 10 mL/min/kg; AUC = 1590 ng·h/mL 3 mg/kg PO: t _{1/2} = 4.6 h; C _{max} = 1,089 ng/mL; AUC = 4920 ng·h/mL; %F = 90
monkey PK ^f	3 mg/kg IV: t _{1/2} = 6.1 h; CL = 0.4 mL/min/kg; V _{ss} = 3.2 L/kg; AUC = 8400 ng·h/mL 10 mg/kg PO: t _{1/2} = 7.3 h; C _{max} = 1660 ng/mL; AUC = 3840 ng·h/mL; %F = 13

^aTransactivation assay. ^bData from Indigo Bioscience assay. ^cData obtained at Aurigene Discovery Technologies Pvt. Ltd. ^dMale CD-1 mice ($n = 3$). ^eMale Wistar rats ($n = 3$). ^fMale cynomolgus monkeys ($n = 3$).

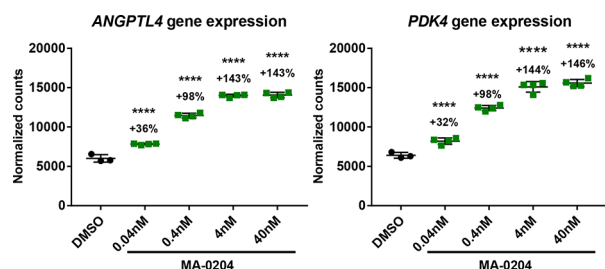


Figure 4. Compound 17 (MA-0204) engages target gene expression in DMD patient muscle myoblast mice (see [Supporting Information](#) for details).

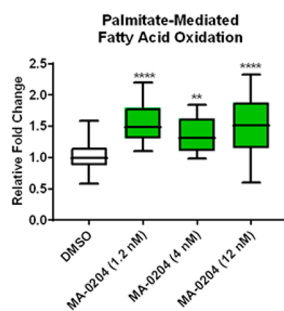


Figure 5. Compound 17 (MA-0204) improves fatty acid oxidation in DMD patient muscle myoblast mice (see [Supporting Information](#) for details).

modulators may offer benefits as a therapeutic strategy for DMD.

■ ASSOCIATED CONTENT

Supporting Information

The Supporting Information is available free of charge on the [ACS Publications website](#) at DOI: [10.1021/acsmchemlett.8b00287](https://doi.org/10.1021/acsmchemlett.8b00287).

Experimental procedures, HPLC and ^1H NMRs, and X-ray crystallographic data ([PDF](#))

■ AUTHOR INFORMATION

Corresponding Author

*Tel: (617)401-9122. E-mail: Bharat.lagu@astellas.com.

ORCID

Bharat Lagu: [0000-0002-2354-3126](https://orcid.org/0000-0002-2354-3126)

Author Contributions

The manuscript was written through contributions of all authors. All authors have given approval to the final version of the manuscript.

Notes

The authors declare the following competing financial interest(s): The authors are current or former employees of Mitobridge, Inc., Astellas Pharma., or Aurigene Discovery Technologies and may have owned or currently own shares of these companies.

■ ACKNOWLEDGMENTS

Authors thank B. Mallesh (Aurigene Discovery Technologies) for technical assistance.

■ ABBREVIATIONS

DMSO, dimethyl sulfoxide; BBr_3 , boron tribromide; DCM, dichloromethane; RT, room temperature; h, hour; $\text{Pd}(\text{PPh}_3)_4$, tetrakis(triphenylphosphine)palladium(0); Na_2CO_3 , sodium

carbonate; DME, 1,2-dimethoxyethane; EtOH, ethyl alcohol; $\text{LiOH}\cdot\text{H}_2\text{O}$, lithium hydroxide monohydrate; THF, tetrahydrofuran; EDCI·HCl, ethylcarbodiimide hydrochloride; HOBt, 1-hydroxy benzotriazole; Et_3N , triethylamine; DMF, N,N -dimethylformamide; $\text{Zn}(\text{OTf})_2$, zinc trifluoromethanesulfonate

■ REFERENCES

- (1) Bushby, K.; Finkel, R.; Birnkrant, D. J.; Case, L. E.; Clemens, P. R.; Cripe, L.; Kaul, A.; Kinnett, K.; McDonald, C.; Pandya, S.; Poysky, J.; Shapiro, F.; Tomezsko, J.; Constantin, C. Diagnosis and management of Duchenne muscular dystrophy, part 1: diagnosis, and pharmacological and psychosocial management. *Lancet Neurol.* **2010**, *9* (1), 77–93.
- (2) Chelly, J.; Kaplan, J. C.; Maire, P.; Gauton, S.; Kahn, A. Transcription of the dystrophin gene in human muscle and non-muscle tissues. *Nature* **1988**, *333*, 858.
- (3) Ryder, S.; Leadley, R. M.; Armstrong, N.; Westwood, M.; de Kock, S.; Butt, T.; Jain, M.; Kleijnen, J. The burden, epidemiology, costs and treatment for Duchenne muscular dystrophy: an evidence review. *Orphanet J. Rare Dis.* **2017**, *12* (1), 79.
- (4) Timpani, C. A.; Hayes, A.; Rybalka, E. Revisiting the dystrophin-ATP connection: How half a century of research still implicates mitochondrial dysfunction in Duchenne Muscular Dystrophy aetiology. *Med. Hypotheses* **2015**, *85* (6), 1021–33.
- (5) Carroll, J. E.; Norris, B. J.; Brooke, M. H. Defective [U- ^{14}C] palmitic acid oxidation in Duchenne muscular dystrophy. *Neurology* **1985**, *35* (1), 96–7.
- (6) Khairallah, M.; Khairallah, R.; Young, M. E.; Dyck, J. R.; Petrof, B. J.; Des Rosiers, C. Metabolic and signaling alterations in dystrophin-deficient hearts precede overt cardiomyopathy. *J. Mol. Cell. Cardiol.* **2007**, *43* (2), 119–29.
- (7) Lin, C. H.; Hudson, A. J.; Strickland, K. P. Fatty acid oxidation by skeletal muscle mitochondria in Duchenne muscular dystrophy. *Life Sci.* **1972**, *11* (7), 355–62.
- (8) Fan, W.; Waizenegger, W.; Lin, C. S.; Sorrentino, V.; He, M. X.; Wall, C. E.; Li, H.; Liddle, C.; Yu, R. T.; Atkins, A. R.; Auwerx, J.; Downes, M.; Evans, R. M. PPARdelta Promotes Running Endurance by Preserving Glucose. *Cell Metab.* **2017**, *25* (5), 1186–1193.
- (9) Peraza, M. A.; Burdick, A. D.; Marin, H. E.; Gonzalez, F. J.; Peters, J. M. The Toxicology of Ligands for Peroxisome Proliferator-Activated Receptors (PPAR). *Toxicol. Sci.* **2006**, *90*, 269.
- (10) Nissen, S. E.; Wolski, K.; Topol, E. J. Effect of Muraglitazar on death and major adverse cardiovascular events in patients with type-2 diabetes mellitus. *JAMA* **2005**, *294* (20), 2581.
- (11) Sznajdman, M. L.; Haffner, C. D.; Malloney, P. R.; Fivush, A.; Chao, E.; Goreham, D.; Sierra, M. L.; LeGrummelec, C.; Xu, E. H.; Montana, V. G.; Lambert, M. H.; Willson, T. M.; Oliver, W. R.; Sternbach, D. D. Novel selective small molecule agonists for peroxisome proliferator-activated receptor delta (PPARdelta)-synthesis and biological activity. *Bioorg. Med. Chem. Lett.* **2003**, *13*, 1517.
- (12) Geiger, L. E.; Dunsford, W. S.; Lewis, D. J.; Brennan, C.; Liu, K. C.; Newsholme, S. J. Rat carcinogenicity study with GW501516, a PPAR delta agonist. *48th Annual Meeting of the Society of Toxicology* **2009**, PS-895.
- (13) Lagu, B.; Kluge, A. F.; Fredenburg, R. A.; Tozzo, E.; Senaiar, R. S.; Jaleel, M.; Panigrahi, S. K.; Tiwari, N. K.; Krishnamurthi, N. R.; Takahashi, T.; Patane, M. A. Novel highly selective peroxisome proliferator-activated receptor delta (PPAR δ) modulators with pharmacokinetic properties suitable for once-daily oral dosing. *Bioorg. Med. Chem. Lett.* **2017**, *27* (23), 5230–5234.
- (14) Lagu, B.; Kluge, A. F.; Goddeeris, M. M.; Tozzo, E.; Fredenburg, R. A.; Chellur, S.; Senaiar, R. S.; Jaleel, M.; Krishna Babu, R. D.; Tiwari, N. K.; Krishnamurthi, N. R.; Takahashi, T.; Patane, M. A. Highly selective peroxisome proliferator-activated receptor delta (PPARdelta) modulator demonstrates improved safety profile compared to GW501516. *Bioorg. Med. Chem. Lett.* **2018**, *28*, 533.
- (15) Wu, C. C.; Baiga, T. J.; Downes, M.; La Clair, J. J.; Atkins, A. R.; Richard, S. B.; Fan, W.; Stockley-Noel, T. A.; Bowman, M. E.; Noel, J.

P.; Evans, R. M. Structural basis for specific ligation of the peroxisome proliferator-activated receptor δ . *Proc. Natl. Acad. Sci. U. S. A.* **2017**, *114*, E2563.

(16) Jorgensen, W. L.; Gao, J. Cis-trans energy difference for the peptide bond in the gas phase and in aqueous solution. *J. Am. Chem. Soc.* **1988**, *110* (13), 4212–4216.

(17) Weiss, M. A.; Jabs, A.; Hilgenfeld, R. H. Peptide bond revisited. *Nat. Struct. Mol. Biol.* **1998**, *5* (8), 676.

(18) Molecular mechanics based energy minimization and conformational analysis study using Molsoft/MMFF force field.

(19) In the transactivation assay CV-1 cells are transfected with a PPAR ligand binding domain fused to a GAL4 promoter to generate a hormone-inducible activator. A test ligand is added and activity is measured in a luciferase assay. See WO2016057660 for further details.

(20) In the protein interaction assay the PPAR ligand complexes with a PPAR ligand binding domain fused to an inactive fragment of galactosidase. This complex complements another inactive galactosidase fragment to form an active galactosidase enzyme that is read out in a fluorescence assay. See www.discoverx.com for details.

(21) Coordinates of the X-ray structure have been deposited in the Protein Data Bank (accession code PDB SZXI).

(22) Batista, F. A. H.; Trivella, D. B. B.; Bernardes, A.; Gratieri, J.; Oliveira, P. S. L.; Figueira, A. C. M.; Webb, P.; Polikarpov, I. Structural insights into human peroxisome proliferator activated receptor delta (PPAR-delta) selective ligand binding. *PLoS One* **2012**, *7*, e33643.

(23) All the animal experiments were carried out as per the guidelines of the Committee for the Purpose of Control and Supervision of Experiments on Animals (CPCSEA), Government of India and approved by the Institutional Animal Ethics Committee (IAEC), Aurigene Discovery Technologies Ltd, Bengaluru, India.